Proceeding of the IEEE
International Conference on Robotics and Biomimetics
Dali, China, December 2019

A Closed Loop Inverse Kinematics and Control Scheme for one Class of Offset-Joint 7-DOF Redundant Manipulator

Yukun Zheng, Hongxiang Yuan, Rui Song*, Xin Ma*, and Yibin Li
Center for Robotics, School of Control Science and Engineering
Shandong University
Jinan 250061, China
{*zhengyk163*}@*163.com*, {*532193056*}@*qq.com*, {*rsong*}@*sdu.edu.cn*, {*maxin*}@*sdu.edu.cn*, {*liyb*}@*sdu.edu.cn*

***Abstract*— This paper presents a position-based motion control method using the closed-loop inverse kinematics (CLIK) algorithm, which is used for solving one class of offset joint 7 degrees of freedom (DOF) robot. Dual-arm robot is one of the research topics in the field of robotics. In the article, we designed a kind of human dual-arm robot with 14-DOF and studied its kinematics with one of the arms. The inverse kinematic can be solved by using the pseudo-inverse matrix, and the numerical solution can be obtained. In the simulation, we adopt position + velocity scheme and at the same time consider the desired orientation as the posture limitation. This algorithm not only can accurately track the target trajectory, but also can avoid the effect of singularity points. Simulation results for one class end biasing 7-DOF robot demonstrates the effectiveness of the scheme, even for singularities.**

***Index Terms*— Closed-loop inverse kinematics, Offset-Joint, Drift-error.**

I. Introduction

Although humanoid robots have been extensively developed and emerged with enhanced performance[1], most humanoid robots can be challenged to overcome their low maneuvering speed. It is still a great challenge to improve the operability and flexibility of humanoid robots. Due to dual-arm robot is more flexible and reliable than the traditional one-arm robot and can completes the requirements of multiple operations, for example, collaborative handling of objects.

Dual-arm robot can effectively complete specific tasks, such as rescue activities[2], aerial work[3,4], robot assembly[5] etc. The current research on humanoid dual-arm robots including: Wu et al.[6] propose a control method for a dual-arm robot for surgical instruments, which the robot is mainly composed of two groups of UR5 manipulators; Peng et al.[7] used three identical double-arm Baxter robots to operate a Shared payload and Qu et al.[8] proposed a redundant dual-arm robot motion learning method based on human-arm coordination characteristics. Garcła et al. adopted the similarity index of cooperative tasks of movements is used to carry out motion planning for a dual-arm robot system composed of two UR robots, which improves the performance of cooperative tasks[9,10]. However, they are usually composed of two 6-DOF robotic arms, which have poor flexibility due to their structural characteristics.

Compared with the 6-DOF robot, the 7-DOF robot has been widely used due to its flexibility advantages brought by redundancy. For example, Talasaz et al.[11] used the dual-arm 14-DOF ABB YuMi robot equipped with a hand-eye RGB camera and then designed a remote robot to provide information to the operator combined with visual-force feedback. The disadvantage of 7-DOF manipulator is that its redundancy makes the number of analytic solutions infinite, which leads to extremely complicated motion control.

At present, many scholars have studied the inverse kinematics of the 7-DOF manipulator. Zhou et al.[12] proposed a practical approach for calculating the analytical inverse kinematic solution of a 7-DOF space manipulator with joint and attitude constraints. Cui et al.[13] proposed a method to solve the inverse kinematics of the manipulator by geometric analysis of the joint position. Lu et al.[14] studied the real-time control of the 7-DOF redundant manipulator by taking advantage of its inverse kinematics.

It is well-known that analytical inverse kinematic solutions exist only for special manipulator geometry, such as the so-called wrist-partitioned type of manipulator. Because the three-axis of the wrist intersect at one point, the robot can be completely decoupled, and the inverse kinematic is relatively simple. However, few studies have carried out inverse kinematics analysis on the mechanism featuring with terminal bias. Due to the offset characteristic of the structure, which is unsolvable in closed-form, several numerical techniques based on the computation of the manipulator's Jacobian matrix are proposed. Xin et al.[15] studied one 7-DOF space manipulator inverse kinematics and used the minimum norm method to choose the best trajectory. Colome A et al.[16] analyzed redundant robot some main concern points, and two

*The paper is supported by Key Research and Development Program of Shandong Province, China(No. 2016ZDJS02A07, No.2017CXGC0915, No.2017CXGC0903-2).

978-1-7281-6321-5/19//$31.00 ©2019 IEEE

improvement to the WAM robot are proposed. Lu S et al.[17] proposed iterative method to solve the inverse kinematics for a specific application scenario. Xu et al.[18] proposed two methods, the joint angle parameterized and arm angle parameterized method, to solve the inverse kinematics for SSRMS type 7-DOF redundant robot with offset configuration. Jiang et al.[19] presented an integrated method in order to obtain the inverse kinematics of the 7-DOF humanoid arm with offset wrist. The simulation results demonstrated the integrated method has better precision and optimization during trajectory tracking.

Recently, we have been developed the new dual-arm robot\dual-manipulators, which is referred to as DUAL-ARM(similar to human arms). In this paper, based on the one-arm in the self-designed 14-DOF dual-arm robot\dual-manipulators which featuring 7-DOF with end biasing mechanism, the inverse kinematics problem based on closed-loop algorithm is studied. In this paper, we present the inverse kinematics solution for the 7-DOF redundant manipulator based on the CLIK algorithm.

This paper is organized as follows. In section II, the kinematics model of the 7-DOF manipulator is presented. In section III, the inverse kinematics analysis is discussed and redundancy resolution at the velocity and acceleration levels are all considered. In section IV, computer simulations are carried out and the section V conclusion and future relate works is described.

II. DUAL-ARMS Robot Structure and Analysis

A. Mechanism Analysis

In this article, the designed DUAL-ARMS robot structure is show in Fig.1(a). It consists of two 7-DOF manipulators, which has seven revolute joints. And in the next work , we only consider the one arm of the robot. The coordinate system of the links is established by D-H method as shown in Fig.1(b). Meanwhile, the D-H parameters of the 7-DOF manipulator are shown in Table 1.

TABLE I
D-H Parameters of 7-DOF Manipulator

i	$a_i(m)$	$\alpha_i(deg)$	$d_i(m)$	$\theta_i(deg)$
1	0	90	0.149	θ_1
2	0.518	0	0.204	θ_2
3	0.428	0	-0.204	θ_3
4	0	-90	0.140	θ_4
5	0	90	0.140	θ_5
6	0	-90	0.140	θ_6
7	0	0	0.082	θ_7

where a_i is the distance between the z_{i-1} and z_i axes along the x_i axis; α_i is the angle from z_{i-1} axis to z_i axis about the x_i axis; d_i is the distance from the origin of frame i-1 to the x_i axis along thez_{i-1} axis; θ_i is the angle between the x_{i-1} and x_i axes about the z_{i-1}axis.

The kinematic structure of the single arm consideration is shown in Fig.1(b). It includes 7 revolute joints that is J1, J2, J3, J4, J5, J6 and J7 , and the joint (actuator) angle values are designated$\theta_1, \theta_2, \theta_3, \theta_4, \theta_5, \theta_6$ and θ_7 correspondingly. Each joint-link pair constitutes one degree of freedom, and hence our manipulator has 7-DOF. These seven variables constitute the joint space. Joints θ_5, θ_6 and θ_7 are referred to as the wrist joints, and are referred to as offset structures because they do not intersect at one point.

For this 7-DOF redundant manipulator, we define coordinate frames 0 to 7 are assigned in Fig.1(b) using the standard D-H method. According to the well know knowledge of homogeneous transformation Denavit-Hartenberg matrix ${}^{i-1}_{i}\mathrm{T}$[20], we can easily obtain the position vector of the end-operator with respect to reference coordinate frame 0. It is called forward kinematics.

$$
\begin{aligned}
{}^{i-1}\mathrm{A}_i &= Trans_z(d_i)Rot_z(\Theta_i)Trans_x(a_i)Rot_x(\alpha_i) \\
&= \begin{bmatrix} c_i & -c\alpha_i s_i & s\alpha_i s_i & \alpha_i c_i \\ s_i & c\alpha_i c_i & -s\alpha_i c_i & \alpha_i s_i \\ 0 & s\alpha_i & c\alpha_i & d_i \\ 0 & 0 & 0 & 1 \end{bmatrix}
\end{aligned} \tag{1}
$$

The Jacobian matrix of the manipulator arm is defined as the linear transformation of its operating velocity and joint velocity, which can be regarded as the transmission ratio of the moving velocity from Joint space to Operating space. Whitney proposed a method, vector product method, to find the robot Jacobian based on the concept of motion coordinate system. For the revolute joint, we can obtain the Jacobian matrix using the following recursive function

$$
J_i = \begin{bmatrix} \nu \\ \omega \end{bmatrix} = \begin{bmatrix} z_i \times {}^{i}\mathrm{p}_0^0 \\ z_i \end{bmatrix} = \begin{bmatrix} z_i \times ({}^{0}_{i}R^{i}\mathrm{p}_i) \\ z_i \end{bmatrix} \tag{2}
$$

Where ${}^{i}p_n^0$ is position vector representation in the base coordinate frame, i.e. the origin of the manipulator coordinate relative to the coordinate system $\{i\}$

$$
{}^{i}p_n^0 = {}^{0}_{i}\mathrm{R}^{i}\mathrm{p}. \tag{3}
$$

Where z_i is the z-axis unit vector in frame $\{i\}$ (expressed in base frame $\{o\}$).

B. Maneuverability

The measure of flexibility and maneuverability is an important part of robot kinematics. The maneuverability is an important indicator of robot flexibility and has been the research object of many scholars. Next we considered the maneuverability of our 7-DOF manipulator. Consider the set of generalized joint velocities with a unit norm

$$
\dot{q}^T \dot{q} = 1. \tag{4}
$$

Where $\dot{q}$ is motion rate of each joints. which locate on the surface of a hypersphere in the seven-dimensional joint

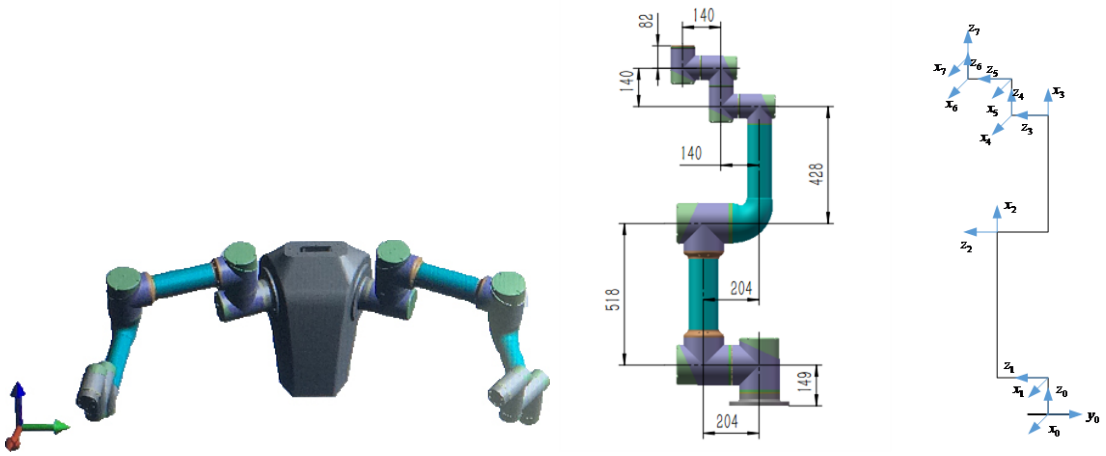

(a) (b)

Fig. 1. The robot structure. (a) The CAD model of DUAL-ARMS robot. (b) The kinematics model of 7-DOF redundant arm.

velocity space. Using the Jacobian matrix can deduce the following manipulability expression

$$\nu^T(J(q)J(q)^T)^{-1}\nu = 1. \tag{5}$$

which is the equation of points on the surface of an ellipsoid within the dim 6-dimensional end-effector velocity space. If this ellipsoid is close to spherical, that is, its radii is of the same order of magnitude then all is well-the end-effector of robot can achieve arbitrary cartesian velocity in the operator space. However, if one or more radii are very small this indicates that the end-effector cannot achieve velocity in the directions corresponding to those small radii.

Using the Yoshikawas manipulability measure method to compute maneuverability named "ellipsoid of maneuverability"[23]. The maneuverability gives a comprehensive measure of the ability of a one-bit robot to move in all directions. Continue the above analysis, thus define manipulability M(q)

$$M(q) = \sqrt{det(J(q)J^T(q))}. \tag{6}$$

A comparison is conducted between PUMA-like robot and our designed robot about manipulability as shown in Fig.2 and it is not difficult to find that our robot prior to PUMA-like robot in the term of manipulability.

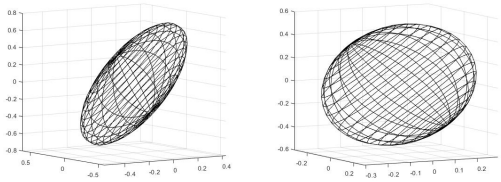

(a) *M(q)*=0.084294 (b) *M(q)*= 0.29117

Fig. 2. End-effector velocity ellipsoids. (a) Velocity ellipsoid for the nominal pose of PUMA-like Robot. (b) Velocity ellipsoid for the nominal pose of our design manipulator.

III. Inverse Kinematics Problem for 7-DOF Manipulator and Closed-Loop Algorithm

For each manipulators we can describe it with a function of time *t* by a position vector *p(t)* and an orientation matrix *R(t)=(n s a)*; where *p* is the vector pointing from a reference base frame to the end frame, and *n, s, a* are the unit director vector of end coordinate system. In this paper, our task is according desired trajectories in the task space to gain the joint space motion. It is said that we assume that a task space trajectory $(x(t), x(\dot{t}))$ is given, and our propose is to find the suitable joint space variable $(q(t), q(\dot{t}))$ in joint space, The direct kinematic equation of manipulators can be describe as

$$X = f(q). \tag{7}$$

This function described the mapping relationship from joint space $q \in R^k$ variable to operational space variable $x \in R^l$. In contrast $x \to q$ is the inverse kinematics. The function expression can be described as formula (8)

$$q = f^{-1}(X). \tag{8}$$

It is well known that Jacobian matrix can depict the relationship of velocity

$$v(t) = \begin{bmatrix} \nu_n \\ \omega_n \end{bmatrix} \Rightarrow \dot{x} = J(q)\dot{q} \tag{9}$$

Where v_n and w_n are 3-column vector describe liner velocity and rotational velocity respectively. We can obtain unique analytical inverse velocity solutions when Jacobian matrix *J(q)* is full ranks

$$\dot{q} = J^{-1}(q)\dot{x}. \tag{10}$$

For 7-DOF redundant manipulators, *J(q)* is not a square matrix, and the Jacobian matrix has 6 Rows and 7 Columns, which is non-full-rank, leading to inverse matrix does not exist. For this problem, the inverse velocity solutions is obtained through using pseudoinverse $J^{\dagger}$ instead of the Jacobian matrix J[21]

$$\dot{q} = J^{\dagger}(q)\dot{x} = J^{T}(JJ^{T})^{-1}\dot{x}. \tag{11}$$

The discrete-time form of motion control scheme can be described with

$$\dot{q}(k) = J^{\dagger}(q(k))\dot{x}. \tag{12}$$

$$\dot{q}(k+1) = q(k) + \triangle t * \dot{q}(k). \tag{13}$$

Where $\triangle t$ is the sample interval and *k* is the sample time series. As all we know that the orientation of end-operator is described by Euler angles (α, β, γ), representing the Roll, Pitch and Yaw angle respectively. The unit vector of the orientation $[^{o}n, ^{o}o, ^{o}a]$ can be derived through the rotation matrix

$$^{A}_{B}\mathrm{R}_{xyz}(\gamma, \beta, \alpha) = \begin{bmatrix} r_{11} & r_{12} & r_{13} \\ r_{21} & r_{22} & r_{23} \\ r_{31} & r_{32} & r_{33} \end{bmatrix} = [^{o}n, ^{o}o, ^{o}a]. \tag{14}$$

Define *e(t)* as a 6×1 error vector, $e(t) = [e_p \ e_o]^T$, are the position error and orientation error respectively. Differentiating *e(t)* to obtain the velocity error $\dot{e}(t)$ and it can be shown that

$$\dot{e}(t) = \begin{bmatrix} \dot{e}_p(t) \\ \dot{e}_o(t) \end{bmatrix} = \begin{bmatrix} \dot{p}_p(t) - \dot{p}(t) \\ \dot{\omega}_p(t) - \dot{\omega}(t) \end{bmatrix} \tag{15}$$

The pseudo-inverse method[22] is used to solve one class of redundant robot, this is desired trajectory tracking problem, but without considered the desired end-operator orientation and it will be yield accumulator of error over time. In order to eliminate the error, however, adding the desired orientation into the control algorithm of trajectory tracking constructed a closed-loop form

$$\dot{q}^{*} \leftarrow J^{\dagger}(q(k))\triangle(q(k), \omega(k)). \tag{16}$$

$$\dot{q}(k+1) = q(k) + K_p \triangle t * \dot{q}(k). \tag{17}$$

Where $\omega(k)$ is the desired pose. In order to improve the control error accuracy of the controller, the addition of PD control has been added. The generalized CLIK algorithm that combines Jacobian pseudo-inverse with PD control can be described as

$$\begin{aligned} \dot{q} &= J^{\dagger}(q)(K_d(\dot{x}_d - \dot{x}) + K_p(x_d - x)) \\ &= J^{T}(JJ^{T})^{-1}(K_d\dot{e} + K_p\dot{e}). \end{aligned} \tag{18}$$

As shown in Fig.3, the control scheme combines the position and velocity control is depicted. The Fig.3(a) depicts a conventional control method that Consider velocity-only feedback. In contrast, the Fig.3(b) we proposed algorithm which including position feedback, velocity feedback and orientation feedback simultaneously.

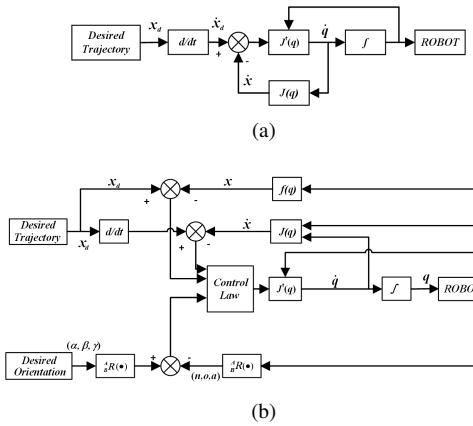

Fig. 3. Two kinds of inverse kinematics algorithm for redundant robot.

IV. Simulations

This section provides the simulation experiments on our 7-DOF robot to validate the effectiveness of the proposed algorithm compare with the velocity-only feedback control scheme.Those simulation are completed in the Matlab/Simulink combined with the Matlab/Robot Toolbox.

A. Simulation 1

In this part, the control algorithm in Fig.3(a) is used to test the following ability of the robot end-effector. First, as shown in Fig.4(a), the construction and control model of a 7-DOF robot was constructed using MATLAB / Simulink. Suppose that the end of the robot moves along an arbitrary curve in the operator space. The desired trajectory equation used is as follows

$$\begin{bmatrix} x = x_0 + 0.4\cos(0.5t) \\ y = y_0 + 0.4\sin(t) \\ z = z_0 + 0.2exp(-0.2t) \end{bmatrix} \tag{19}$$

$$q = [0, 1.0472, -0.5236, -2.0944, 0, 1.5708, -1.5708]$$

Where (*x*, *y*, *z*) and (x_0, y_0, z_0) are the desired trajectory and the initial position of the robot respectively. q is the joint angles of the initial pose of the robot, and the current position and orientation of the robot can be obtained by transformation matrix formula(14) using these initial joint angles. The spatial curve experiment is performed using a control method with only speed feedback, and the trajectory tracking is shown in Fig.4(b). As can be seen from the figure, the deviation between the two curves is obvious, and there is an accumulation of errors. Fig.4(c) is an error curve between the two curves, which better reflects the accumulation of errors.

B. Simulation 2

This section, the proposed control algorithm will be tested in 3D space, and the desired trajectory used is as follows

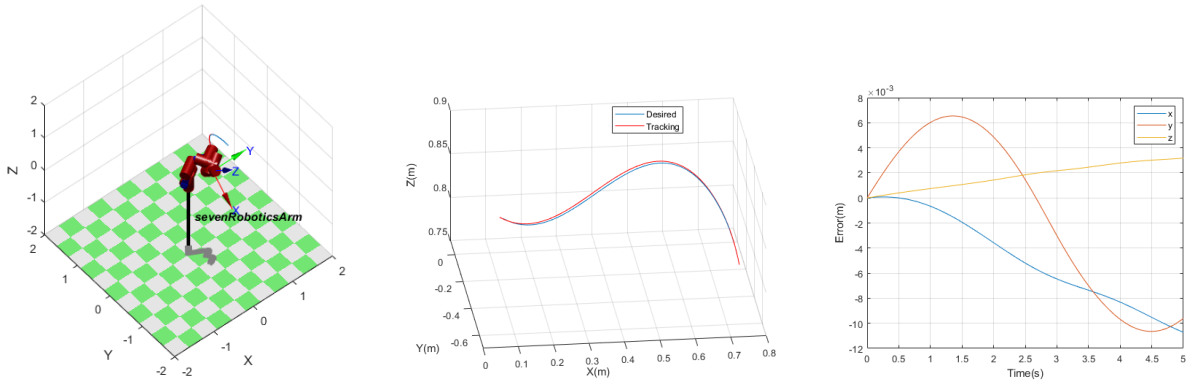

(a) (b) (c)

Fig. 4. Robot model and tracking curve.(a) The robot model, (b) The desired trajectory and tracking trajectory. (c) Tracking error of the end effector.

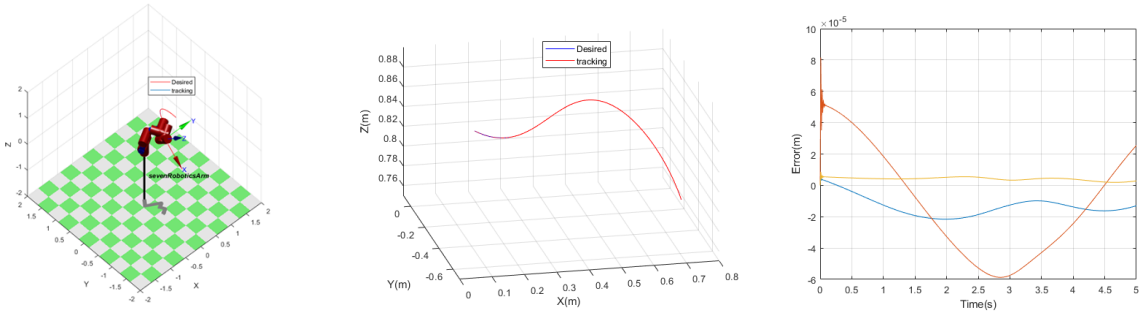

(a) (b) (c)

Fig. 5. Trace curve simulation results.(a) and (b) The desired trajectory and tracking trajectory. (c) Tracking error of the end effector.

$$\begin{bmatrix} x = x_0 + 0.4\cos(0.5t) \\ y = y_0 + 0.4\sin(t) \\ z = z_0 + 0.2exp(-0.2t) \end{bmatrix} \tag{20}$$

$$q = [0, 1.0472, -0.5236, -2.0944, 0, 1.5708, -1.5708]$$

Fig.5 shown the tracking trajectory of the end-operator and the error curves for the end coordinates. As we can see form Fig.5.(a) and (b), robot end-operator can track the desired trajectory effectively. Fig.5.(c) is shown the error curves, its accuracy up to 0.01mm. It is better than frist controller.

V. Conclusion and Future Works

This paper introduces a new structure dual-arms robot, which has 14-DOF and consists of two manipulators with 7-DOF. Different from the traditional robot, it has a terminal three-axis offset mechanism. The inverse solution algorithm for one class end-biasing robot which last three axes of end manipulator are not intersect one point is obtained based on velocity control and accelerated velocity control. To avoid the drifting errors, orientation control method has been added. In the section 4, we conduct two sets of simulation experiments to verify corrective and performance of the proposed algorithm. Simulations show that the robot has good performance used our proposed algorithm. The method can achieve accurate trajectory tracking without increasing the time complexity of the algorithm.

In this paper, we only considered the one arm of DUAL-ARM robot. Because the two arms of the robot are the same. In the future work, we will aim to complete the whole robot structure; to test its cooperatively ability of double arms; to design a robust and adaptive controller using force control which can effectively interact with environment.

References

[1] G. Pratt, J. Manzo, "The DARPA Robotics Challenge," IEEE Robotics and Amp Automation Magazine, 20(2):10-12, 2013.

[2] B, Choi, G. Park, and Y. Lee, "Practical control of a rescue robot while maneuvering on uneven terrain," Journal of Mechanical Science and Technology. 2018, 32(5), 2021-2028

[3] V. Lippiello, G. A. Fontanelli, and F. Ruggiero, "Image-Based Visual-Impedance Control of a Dual-Arm Aerial Manipulator," IEEE Robotics and Automation Letters, vol. 3, no. 3, pp. 1856-1863, 2018.

[4] A. Suarez, G. Heredia, and A. Ollero, "Physical-Virtual Impedance Control in Ultralightweight and Compliant Dual-Arm Aerial Manipulators," IEEE Robotics and Automation Letters, vol. 3, no. 3, pp. 2553-2560, 2018.

[5] M. Young, The Technical Writer's Handbook, Mill Valley, CA: University Science, 1989.

[6] Q. Wu, M. Li, X. Qi, Y. Hu, B. Li, and J. Zhang, "Coordinated control of a dual-arm robot for surgical instrument sorting tasks," Robotics and Autonomous Systems, vol. 112, pp. 1-12, 2019.
[7] Y.-C. Peng, D. S. Carabis, and J. T. Wen, "Collaborative manipulation with multiple dual-arm robots under human guidance," International Journal of Intelligent Robotics and Applications, vol. 2, no. 2, pp. 252-266, 2018.
[8] J. Qu, F. Zhang, Y. Wang, and Y. Fu, "Human-like coordination motion learning for a redundant dual-arm robot," Robotics and Computer-Integrated Manufacturing, vol. 57, pp. 379-390, 2019.
[9] N. Garcia, R. Suarez, and J. Rosell, "Task-Dependent Synergies for Motion Planning of an Anthropomorphic Dual-Arm System," (in English), Ieee Transactions on Robotics, vol. 33, no. 3, pp. 756-764, Jun 2017.
[10] N. Garcia, J. Rosell, and R. Suarez, "Motion Planning by Demonstration WithHuman-Likeness Evaluation forDual-Arm Robots," IEEE Transactions on Systems, Man, and Cybernetics: Systems, vol. PP, no. 99, pp. 1-10, 2017
[11] D. Nicolis, M. Palumbo, A. M. Zanchettin, and P. Rocco, "Occlusion-Free Visual Servoing for the Shared Autonomy Teleoperation of Dual-Arm Robots," IEEE Robotics and Automation Letters, vol. 3, no. 2, pp. 796-803, 2018.
[12] D. Zhou, L. Ji, Q. Zhang, and X. Wei, "Practical analytical inverse kinematic approach for 7-DOF space manipulators with joint and attitude limits," Intelligent Service Robotics, vol. 8, no. 4, pp. 215-224, 2015.
[13] C. Z. and H. Z. J., "Inverse Kinematics Algorithm of 7-DOF Manipulator Based on Self-Motion," Journal of Shanghai University, vol. 18, no. 06, pp. 589-595, 2012.
[14] H. Lu, X. Zhou, and R. Li, "An optimization algorithm for trajectory planning of a 7-DOF redundant manipulator," in Navigation and Control Conference, 2017: IEEE.
[15] P. Xin, J. Rong, Y. Yang, and D. Xiang, "Inverse Kinematics Analysis of a 7-DOF Space Manipulator for Trajectory Design," Journal of Beijing Institute of Technology, vol. 26, no. 03, pp. 285-291, 2017.
[16] A. Colome and C. Torras, "Closed-Loop Inverse Kinematics for Redundant Robots: Comparative Assessment and Two Enhancements," IEEE/ASME Transactions on Mechatronics, vol. 20, no. 2, pp. 944-955, 2015.
[17] S. Lu, Y. Gu,J. Zhao, and L. Jiang, "An Iterative Calculation Method for Solve the Inverse Kinematics of a 7-DOF Robot with Link Offset," International Conference on Intelligent Robotics and Applications, 2017.
[18] W. F. Xu, J. T. Zhang, L. Yan, and Z. Y. Wang, "Parameterized inverse kinematics resolution method for a redundant space manipulator with link offset," Journal of Astronautics, vol. 36, no. 1, pp. 33-39, 2015.
[19] L. Jiang, X. J. Huo, Y. W. Liu, and H. Liu, "An Integrated Inverse Kinematic Approach for the 7-DOF Humanoid Arm with Offset Wrist," (in English), 2013 Ieee International Conference on Robotics and Biomimetics (Robio), pp. 2737-2742, 2013.
[20] C.-H. Lee, J. Choi, H. Lee, J. Kim, K.-m. Lee, and Y.-b. Bang, "Exoskeletal master device for dual arm robot teaching," Mechatronics, vol. 43, pp. 76-85, 2017.
[21] S. R. Buss, "Introduction to inverse kinematics with jacobian transpose, pseudoinverse and damped least squares methods," IEEE Journal of Robotics and Automation, vol. 17, no. 1, 2004.
[22] J. G. Wang, Y. M. Li, and X. H. Zhao, "Inverse Kinematics and Control of a 7-DOF Redundant Manipulator Based on the Closed-Loop Algorithm," (in English), International Journal of Advanced Robotic Systems, vol. 7, no. 4, pp. 1-9, Dec 2010.
[23] T, Yoshikawa, "Manipulability of Robotic Mechanisms," The International Journal of Robotics Research, 4(2),3-9. 1985.